COMPUTER METHODS IN APPLIED MECHANICS AND ENGINEERING 19 (1979) 151–158

A PRACTICAL METHOD FOR LIMIT TORSION PROBLEMS

Wei H. YANG

Department of Applied Mechanics and Engineering Science,
The University of Michigan, Ann Arbor, Michigan, U.S.A.

The sand hill analogy should have closed the chapter of the limit plastic torsion problem except that there exists no convenient method to evaluate the volume of a general sand hill which gives the limiting torque. Consequently, only a few solutions of practical importance appear in the literature. A finite element method is developed to facilitate accurate and efficient integration of the volume. The method applies to prismatic torsion bars of a general cross-section. Four new solutions are presented for elliptical and grooved circular shafts as well as cracked rectangular and circular shafts. An inconsistency resulting from nonuniform convergence in a limiting case of the elastic solution of the grooved shaft is removed from the corresponding plastic solution. The stresses in the cracked shafts are bounded in the plastic solutions, providing a different way of estimating the failure torque from the fracture mechanics predictions.

1. Introduction

The limit analysis of plastic structures [1] as well as continuum [2] has the value of providing quick and adequate estimates of the bounds on the more elaborate elastic and elastoplastic solutions. The theorems of the limit analysis are well established. But the methods of solution are not and are in need of improvement. The issue here is not the capability and feasibility of a solution. It is the efficiency and convenience of a method in terms of the human effort of setting up a problem and the computer time and memory requirement for its solution that can enhance the usefulness of the limit analysis. Without a general and fast method the value of the limit analysis is greatly diminished.

It has long been recognized that mathematical programming methods are applicable to the limit analysis [3]. Many research papers [4]–[6] have been devoted to the marriage of the two fields. The trend seems to be in the direction from the theoretical study of the limit analysis to the theoretical study of the related mathematical programming problems. There are only a few papers devoted to computational implementation of these well-studied theoretical analyses. In the opinion of this author the limit analysis will be useful to engineers only if algorithms and computer programs are made available that handle easily the complicated boundary value problems.

In this paper, only the limit analysis of the plastic torsion problem is discussed. A mathematical formulation of the problem is stated below. Let $\phi(x, y)$ be the stress function for the stresses σ_{zx}, σ_{zy} in the cross-section of the prismatic bar shown in fig. 1 such that

$$\sigma_{zx}/\sigma_0 = \partial\phi/\partial y, \quad \sigma_{zy}/\sigma_0 = -\partial\phi/\partial x, \tag{1}$$

where the stresses are made dimensionless by normalizing with respect to the yield stress σ_0. Obviously, $\phi(x, y)$ satisfies the equilibrium equation. It is a lower bound solution if the yield criterion $|\nabla\phi(x, y)| \leqslant 1$ is not violated [2].

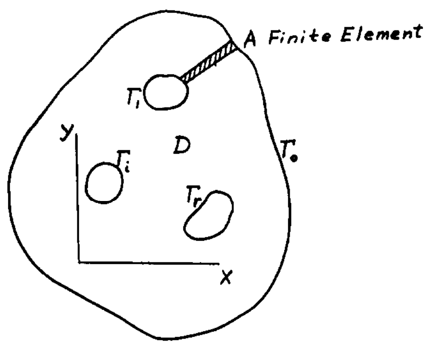

Fig. 1. A general cross-section of a prismatic bar.

The limit torque is given by the solution of the optimization problem (see [7]):

$$T = 2 \iint_D \phi(x, y)\mathrm{d}A$$

maximize
subject to

$$\begin{aligned} & |\nabla \phi| \leqslant 1 \text{ in } D, \\ & \phi = 0 \text{ on } \Gamma_0, \\ & \phi = C_i \text{ on } \Gamma_i, \quad i = 1, 2, \ldots, \\ & \phi(x, y) \text{ is continuous in } D. \end{aligned} \tag{2}$$

where T is the torque, Γ_0 is the outer boundary of the cross-section, Γ_i are the boundaries of holes in the domain D bounded by Γ_0, and C_i are constants. It can be shown that the optimal solution of (2) will drive the yield criterion to its upper bound $|\nabla\phi(x, y)| = 1$. Geometrically, the solution is a surface of constant absolute slope analogous to a sand hill [2]. It should be noted that the surface may have discontinuous derivatives along a finite number of curves or lines in the domain known as the ridge lines of the sand hill. Although the solution can be constructed geometrically, there exist no convenient method to integrate the stress function which gives the limiting torque.

A special finite element scheme is developed to facilitate the integration. Since the stress function is linear along one direction, narrow and long elements are chosen along these steepest descent directions between the ridge lines and the boundaries. The order of approximation depends only on the mesh size along the contours of the stress function.

Two families of cross-sections which have exact elastic solutions are chosen for the limit plastic analysis. They are ellipses and grooved circles. In the limiting case when the groove dimension approaches zero the elastic solution does not approach the solution for the circular shaft without the groove. The plastic solution of the grooved shaft however converges uniformly to that without the groove. The solutions of cracked rectangular and circular shafts are also presented for the entire range of crack extensions.

2. Finite element method

The finite element method is a very powerful tool for numerical integration [8]. When the smoothness properties of the integrand are known, special finite element schemes can be developed to optimize the order of approximation. In the case of the limit plastic torsion problem the linearity of the stress function along steepest descent directions suggests the use of long and narrow elements along these directions, as shown in fig. 1. A complete analysis of this type of elements is given by Laskin and Yang [9]. To present the idea simply, triangular elements with linear interpolation functions are used in this paper. The integration error using these elements is $O(h)$. A sufficiently small mesh size h is chosen so that the integration error is the same order of magnitude as that of the round-off errors. Since the small mesh is taken only in one direction, computing time increases only linearly with the inverse fo the mesh size $1/h$.

A triangular element spans the space between two boundaries or between a boundary and a ridge line. One of the long edges of the triangle coincides with a steepest descent direction. It is this type of mesh configuration that makes calculations of the limit torque simple and efficient. The stress function is approximated by a linear function within the element. The torque has the form

$$T = 2 \iint_D \phi(x, y)\mathrm{d}A = 2 \sum \iint_\Delta \phi(x, y)\mathrm{d}A = \sum \tfrac{2}{3}(\phi_i + \phi_j + \phi_k)A_{ijk} + O(h), \tag{3}$$

where A_{ijk} is the area of the triangle with its vertices at mesh points i, j and k, and the summation is taken over the domain consisting of all triangles. The area can be expressed in terms of the coordinates of the vertices:

$$A_{ijk} = \text{one-half the absolute value of the determinant} \begin{vmatrix} 1 & x_i & y_i \\ 1 & x_j & y_j \\ 1 & x_k & y_k \end{vmatrix} . \tag{4}$$

A point on the ridge line, where the normal derivative of the stress function is discontinuous, is the intersection of at least two lines along the steepest descent directions. It has equal distance to the boundary points following each steepest descent direction. This distance is also the value of the stress function at the point. These points (and thus the ridge lines) can be located by solving a few nonlinear algebraic equations of the boundaries. The ridge line calculations are problem-dependent, as shall be described in the next two sections.

An isoparametric element that has $O(h^3)$ error and treats the curved boundary with the same order of approximation is given in [9]. The higher accuracy is gained at the expense of added effort in programming and data preparation when setting up a problem for computation. For a large problem the advantage of this higher order element may well be worth the effort. The question of the optimal order of approximation will not be addressed in this paper.

3. Elliptical shaft

A family of elliptic shafts with various ratios of minor and major axes are chosen for the plastic torsion analysis. There exist exact elastic solutions [10] as well as plastic solutions [11] for these cross-sections.

The major and minor semiaxes of the ellipse are denoted by a and b, respectively. The ridge line is a segment along the major axes. The steepest descent direction from a point $(\xi, 0)$ on the ridge line to a point (x, y) on the elliptic boundary must be normal to the boundary at (x, y). This condition can be stated as

$$[y/(x-\xi)]\,[-bx/a\sqrt{a^2-x^2}] = -1. \tag{5}$$

Solving (5) with the use of the equation of the ellipse $(x/a)^2 + (y/b)^2 = 1$, we obtain the parametric form

$$x = a^2\xi/(a^2-b^2), \quad y = b\sqrt{1 - a^2\xi^2/(a^2-b^2)} \tag{6}$$

of the point (x, y) associated with $(\xi, 0)$ on the ridge line. The equations in (6) are used to generate a mesh system shown in the left halves of the figures in fig. 2. A family of curves which are orthogonal to the mesh lines is shown in the right halves. Each quadrilateral mesh unit is divided into two triangles by a diagonal. From the first equation of (6) the terminating points of the ridge line are determined. They are at $\pm(1 - b^2/a^2)a$. Near the two ends of the ellipse the stress function behaves in a form similar to a conical surface with the vertex at the end points of the ridge line. The integration over the curved end element is approximated by the volume of a cone.

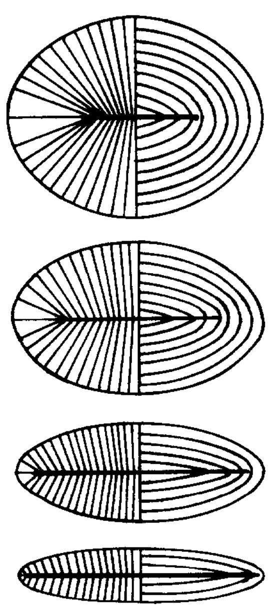

Fig. 2. Elliptical cross-sections.

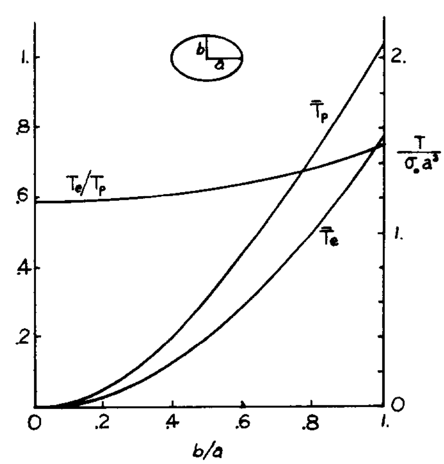

Fig. 3. Elastic and plastic torque curves for the elliptical shafts.

The dimensionless torque $T/(\sigma_0 a^3)$ is calculated by the finite element integration. For various b/a ratios the plastic solutions are compared with the elastic solutions indicating the safety margins of the maximum elastic torque for ductile materials. The results are shown in fig. 3. The computed plastic solutions agree with the analytic solutions given by formula (4.8) in [11].

4. Grooved circular shaft

An interesting elastic solution of a grooved circular shaft is given in [10]. When the radius of the groove b is small compared to the radius of the shaft a, the elastic solution has an inconsistency. As b approaches zero, the maximum elastic torque is only half that of an identical shaft without the groove. This phenomenon occurs often in the theory of elasticity known as nonuniform convergence in the limit.

In the coordinate system shown in fig. 4 let the point (ξ, η) on the ridge line be associated by two steepest descent directions with the point (x, y) on the circle and the point (u, v) on the groove. The three points satisfy the relations

$$\begin{aligned} &\eta/\xi = v/u, \\ &\eta/(a-\xi) = y/(a-x), \\ &u^2 + v^2 = b^2, \\ &(a-x)^2 + y^2 = a^2, \\ &(x-\xi)^2 + (y-\eta)^2 = (u-\xi)^2 + (v-\eta)^2 . \end{aligned} \tag{7}$$

Eliminating x, y, u and v from the system of equations above, the ridge equation

$$a[\sqrt{(\xi-a)^2+\eta^2} - \xi] - b\sqrt{\xi^2+\eta^2} = a^2 - b^2/2 \tag{8}$$

is obtained.

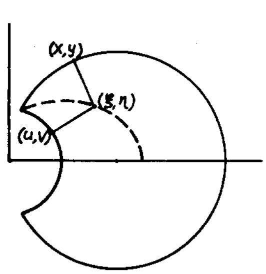

Fig. 4. Coordinate definitions of the grooved circular shaft.

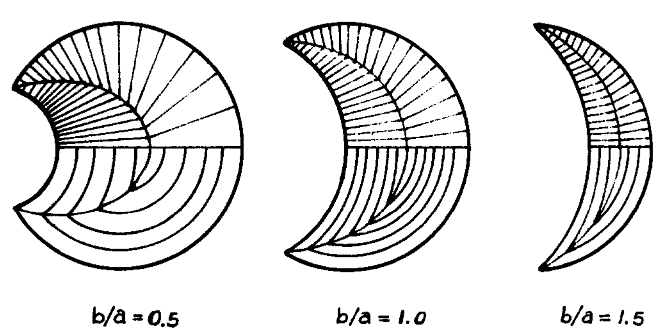

Fig. 5. Grooved circular cross-sections.

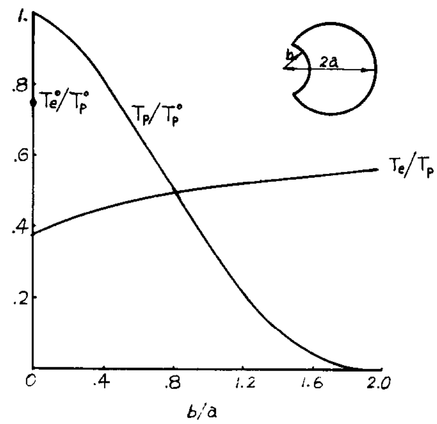

Fig. 6. Elastic and plastic torque curves for the grooved circular shafts.

The grooved cross-sections for three b/a ratios are shown in fig. 5. The top halves of the figures show the finite element mesh lines, while the bottom halves show the contour curves of the stress function.

The finite element integration gives the limit plastic torque T_p. The solutions for various b/a ratios are shown in comparison with the maximum elastic torque T_e in fig. 6. The limit plastic torque and the maximum elastic torque for a circular shaft without the groove are denoted by T_p^0 and T_e^0, respectively. The ratio T_e/T_p as b/a approaches zero converges to half of the value given by T_e^0/T_p^0 shown by the dot in the figure. The limit plastic torque T_p however converges uniformly to T_p^0 as b/a approaches zero.

5. Cracked shafts

Elastic solutions of cracked shafts [12] have been used extensively for predictions of fracture load. The limit plastic solutions of cracked shafts, which could serve as upper bounds for the fracture load, have been somehow overlooked.

Using the finite element method presented, the limit torques of cracked rectangular and circular shafts can be easily obtained. The cross-sections of the cracked shafts with different crack extensions are shown in fig. 7. Again, the top halves of the figures show the finite element mesh lines, while the bottom halves show the contour curves of the stress functions.

The ridge line calculations are similar to the cases presented, and their discussions are omitted here. The limit torques of the rectangular and circular shafts for the entire range of crack extension ratios are presented in fig. 8.

The shear stresses at the tips of the cracks are of course bounded from the inequality condition in (2). This requires superductility of the materials. It should be noted here that superplastic materials do exist and are under active research and development. For moderately ductile materials the solutions presented here may serve as close upper bounds.

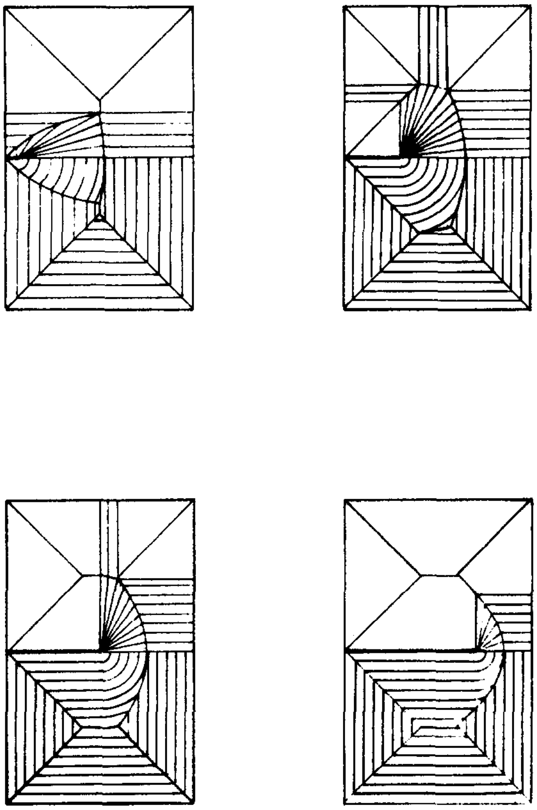

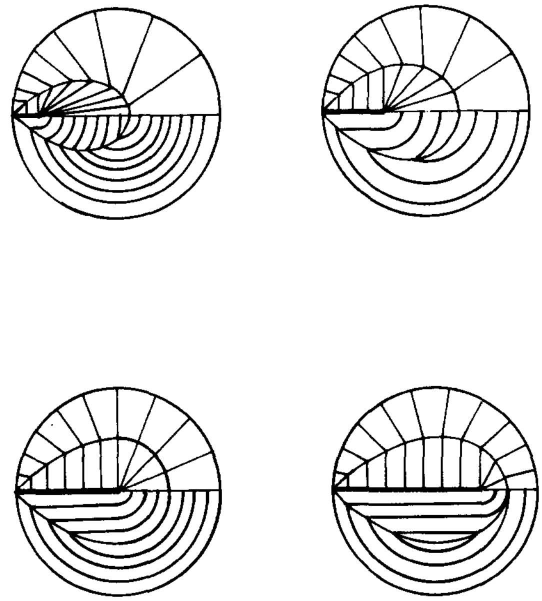

Fig. 7a. Cracked rectangular cross-sections.
Fig. 7b. Cracked circular cross-sections.

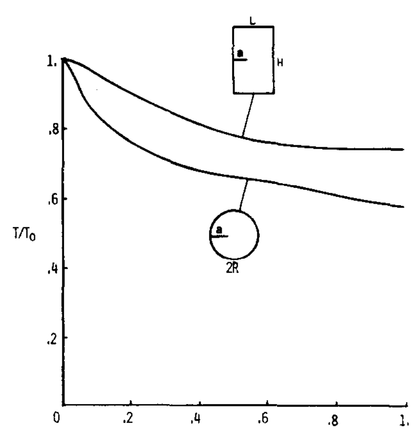

Fig. 8. Plastic torque curves for cracked shafts.

6. Final remarks

Limit plastic solutions are upper bounds of elastic and elastoplastic solutions. For ductile materials the limit analysis solutions are quite realistic. The method presented here should handle at ease the limit torsion problem of a general cross-section. A two-dimensional integration problem is reduced to essentially a scalar integration similar to the trapezoidal rule. This one-dimensional nature makes the optimal order of approximation a secondary consideration. Even with the simple linear $O(h)$ approximation used in this paper the computing time for the exhaustive parameter variation on the four problems presented amounts to less than two minute CPU (Amdahl 470) time with single precision arithmetic. The $O(h^3)$ method mentioned earlier will further reduce the already quite acceptable computing cost.

The sensitivity of some linear elastic solutions to small geometric perturbations is well known. The infinitesimal groove simulates a hair-line scratch on the surface of the shaft. For a highly brittle material this scratch may greatly affect the torsional capacity of the shaft. This is a subject of great interest in fracture mechanics. For ductile materials like metals such sensitivity can be dubious. Singular elastic stress fields around the crack tips have been used widely in fracture mechanics analysis. For ductile materials, predictions of fracture strength from such analysis are inaccurate. It is suggested here that the limit analysis may offer bounds for fracture mechanics analysis of ductile materials.

Acknowledgment

The author is grateful for the partial support by NSF grant Eng 75-17489.

References

[1] P.G. Hodge Jr., Plastic analysis of structures (McGraw-Hill, 1959).
[2] W. Prager and P.G. Hodge Jr., Theory of perfectly plastic solids (Wiley, 1951).
[3] J.D. Foulkes, Minimum weight design and the theory of plastic collapse, Q. Appl. Math. 10 (1953) 347–358.
[4] J.B. Martin, Plasticity: fundamentals and general results (MIT Press, 1975).
[5] J.C. Nagtegaal, D.M. Parks and J.R. Rice, On numerically accurate finite element solutions in the fully plastic range, Comp. Meths. Appl. Mech. Eng. 4 (1974) 153–177.
[6] NATO Advanced Study Institute on Engineering Plasticity and Mathematical Programming, Univ. Waterloo, Ont., Canada, Aug. 2–12, 1977.
[7] L. Watson and W.H. Yang, On a class of optimization problems in continuum mechanics, Comp. Meths. Appl. Mech. Eng. 15 (1978) 353–364.
[8] P.G. Ciarlet, Numerical analysis of the finite element method (Les Presses de l'Universite de Montreal, 1976).
[9] M. Luskin and W.H. Yang, A special $O(h^3)$ finite element for limit plastic analysis (AMES Report 17-2-78, Univ. Michigan, Ann Arbor, MI, 1978).
[10] S. Timoshenko and J.N. Goodier, Theory of elasticity, 3rd ed. (McGraw-Hill, 1970).
[11] W. Olszak, P. Perzvna and A. Sawczuk (eds.), Theory of plasticity [Polish] (PWN, Warsaw, 1965).
[12] R. Westmann and W.H. Yang, Cracked rectangular beams, J. Appl. Mech. 34 (1976) 693–701.